Published in final edited form as:
Cancer Biol Ther. 2009 November ; 8(22): 2194–2205.

Visualization and enrichment of live putative cancer stem cell populations following p53 inactivation or Bax deletion using non-toxic fluorescent dyes

Joshua E. Allen[1,2], **Lori S. Hart**[1], **David T. Dicker**[1], **Wenge Wang**[1], and **Wafik S. El-Deiry**[1,2,*]

[1]Laboratory of Molecular Oncology and Cell Cycle Regulation; Departments of Medicine (Hematology/Oncology), Genetics and Pharmacology; the Institute for Translational Medicine and Therapeutics; and the Abramson Comprehensive Cancer Center

[2]Biochemistry and Molecular Biophysics Graduate Group; University of Pennsylvania School of Medicine; Philadelphia, PA USA

Abstract

Putative cancer stem cell (CSC) populations efflux dyes such as Hoechst 33342 giving rise to side populations (SP) that can be analyzed or isolated by flow cytometry. However, Hoechst 33342 is highly toxic, more so to non-SP cells, and thus presents difficulties in interpreting in vivo studies where non-SP cells appear less tumorigenic than SP cells in immunodeficient mice. We searched for non-toxic dyes to circumvent this problem as well as to image these putative CSCs. We found that the fluorescent dye calcein, a product of intracellular Calcein AM cleavage, is effluxed by a small subpopulation, calcein low population ($C^{lo}P$). This population overlaps with SP and demonstrated long term cell viability, lack of cell stress and proliferation in several cancer cell lines when stained whereas Hoechst 33342 staining caused substantial apoptosis and ablated proliferation. We also found that the effluxed dye D-luciferin exhibits strong UV-fluorescence that can be imaged at cellular resolution and spatially overlaps with Calcein AM. In order to evaluate the hypothesis that p53 loss promotes enrichment of putative CSC populations we used Calcein AM, D-luciferin and Mitotracker Red FM as a counterstain to visualize dye-effluxing cells. Using fluorescence microscopy and flow cytometry we observed increased dye-effluxing populations in DLD-1 colon tumor cells with mutant p53 versus wild-type (WT) p53-expressing HCT116 cells. Deletion of the wild-type p53 or pro-apoptotic Bax genes induced the putative CSC populations in the HCT116 background to significant levels. Restoration of WT p53 in HCT116 $p53^{-/-}$ cells by an adenovirus vector eliminated the putative CSC populations whereas a control adenovirus vector, Ad-LacZ, maintained the putative CSC population. Our results suggest it is possible to image and quantitatively analyze putative CSC populations within the tumor microenvironment and that loss of pro-apoptotic and tumor suppressing genes such as Bax or p53 enrich such tumor-prone populations.

Keywords

cancer stem cells; p53; Hoechst 33342; Calcein AM; Bax; colon cancer; microscopy; flow cytometry; side population; calcein low population

*Correspondence to: Wafik S. El-Deiry; wafk@mail.med.upenn.edu .

Introduction

The notion that cancer emanates from a small subpopulation of cells which possess the ability to self renew as well as differentiate was first suggested over 150 years ago.1 Since then, empirical evidence has amassed to buttress this theory including the identification of a small subset of cells isolated from tumor tissues which contained a pronounced capacity to proliferate under in vivo conditions.2,3 To explore the alternative explanation that all cancer cells simply have a low probability of clonogenicity, one study isolated cancer cells from acute myeloid leukemia (AML) tissue samples and sorted for populations expressing $CD34^+/ CD38^-$, mammalian cell surface glycoproteins which are putative CSC markers found in AML.4,5 The subpopulation possessing the aforementioned marker properties indeed possessed an exclusive and potent potential to transfer AML from humans to NOD/ SCID mice.[6] Corroboration of the CSC theory has expanded to include animal models and other CSC markers such as CD133 (PROM1)[7] and $CD44^+/CD24^-$,8 in brain and breast solid tumors, respectively. These attributions of self renewal and differentiation potential in conjunction with the manipulation of normal cellular regulatory processes give rise to a cogent putative mechanism of the unique tumorigenicity of CSC and its suggested role in metastasis. Functional properties of putative CSC populations have also been noted such as increased aldehyde dehydrogenase (ALDH) activity[9] and dye-efflux which gives rise to side populations (SP).10

SP cells are a small subset of a cellular population initially identified in murine bone marrow by flow cytometry due to their efflux of the fluorescent dye Hoechst 33342.11 This efflux property has been ascribed to the ATP binding cassette (ABC) transporters,[12] including P-glycoprotein (P-gp) as well as ABCG2, and identification of these subpopulations is qualified by inhibiting the SP efflux via ABC transporter inhibitors such as verapamil. P-gp is encoded by the MDR1 gene which has been shown to be transcriptionally regulated by Ras and p53.13 This regulation has been found to be disrupted upon p53 mutation in vivo and has been extended to MRP1 as well.14–16 Further studies have also revealed a relationship of inactivating pro-apoptotic genes p53 or INK4a in addition to overexpressing the anti-apoptotic Bcl-2 with increased resistance to chemotherapy in vivo.17–19 The substrates of ABC transporters include small molecule chemotherapeutic agents such as topotecan,20 methotrexate,21 paclitaxel22 and Imatinib mesylate[23] thus implicating SP cells in multidrug resistance (MDR).[24] SP cells have been characterized in several cancer cell lines and in primary tumor samples of mesenchymal neoplasms,25 neuroblastomas,12 as well as ascites of ovarian cancers.26 Continuing research on the identification of SP cell properties has yielded an imperfect but clearly recognizable overlap with that of various stem cell markers. Such overlapping properties have been found in murine tissues including the majority of isolated SP cells expressing CD45 in bone marrow,[27] CD34 in skin tissue,[28] Sca-1 in bone marrow,[29] skeletal tissue,[30] mammary gland,[31] testis[32] and skin tissue,[33] as well as c-kit in brain tissue[34] and bone marrow.[29]

Disparities between properties identified from putative CSCs and SP cells are inherent for a few reasons. First of all, SP cells have been shown to be sensitive to variables such as method of preparation, confluency, hypoxia and serum levels which sensitizes isolation to inconsistency across samples.[35] Additionally, SP cells as well as putative CSCs are identified based on an operational definition, e.g., cell surface markers, which may contribute to the phenotype but not exclusively confer it. For instance, SP cells are identified by their efflux property which has been attributed to ABC transporters such as ABCG2 and have been shown to be tumorigenic in nude mice.[36] However, $ABCG2^+$ and $ABCG2^-$ SP cells, while both are more tumorigenic than non-SP cells, have been shown to have similar tumorigenicity.[37]

Hoechst 33342 is known to inhibit DNA topoisomerase I in addition to increasing levels of ATM, Chk2 and p53 phosphorylation.[38,39] A change in γH2AX is also noted and is thought

to occur as a result of Hoechst 33342 binding to the minor groove of DNA which alters chromatin structure.40 Importantly, despite the significant efflux of the dye in stem cells, it has been shown that stem cells still retain 10–80% of Hoechst 33342 relative to non stem cells.11,[41] At exposures of 18 h to Hoechst 33342 (1 μM), cells arrest in G_2 and exhibit significantly increased levels of activated ATM, activated Chk2 and phosphorylated p53(Ser15).[39] It should also be noted that these observations were made at a concentration 10-fold less than the prototypical staining concentration recommended for SP analysis by flow cytometry (5 μg/mL).11 As Hoechst 33342 clearly alters protein expression levels, cellular properties are likely to be differentially affected throughout the population. Using Hoechst 33342 staining as a sorting method for tumorigenicity studies is also confounded by the toxicity of Hoechst 33342 which strongly influences proliferation. Therefore an alternative method of identifying subpopulations with this putative CSC efflux property in a non-toxic manner is warranted and would potentially allow for longitudinal and/or in vivo studies without altering cell properties. Such studies have the potential to dispel the small but persistent empirical disparities between CSC and SP cells.

Visualizing live CSCs in cell culture and in vivo holds great value for understanding cancer pathogenesis, metastasis, resistance to therapy and the development of novel therapies targeting CSCs within the tumor microenvironment. Current methods for identifying CSCs typically involve sorting by flow cytometry or immunohistochemical staining for putative CSC marker properties. A significant limitation of these approaches is that they cannot be performed in vivo as they require the removal of cells from their natural environment for analysis and in some cases fixation of the cells so that they are no longer viable. Visualizing live CSCs via a noninvasive, non-toxic stain would provide a window to observe CSCs in a more biologically and clinically relevant environment, possibly in vivo. Several studies have employed dyes to differentiate between SP cells and non-SP cells including luciferin assays for determining ABCG2 inhibitors.[42] Interpretation of such experiments is subject to caution due to the possibility of displaying altered properties due to dye-retention and not physiological properties. The ensuing method allows for visualization of putative CSCs and extends as a tool for clarification of these ambiguities.

To address these concerns, we propose calcein as an alternative fluorescent dye to Hoechst 33342 due to its similar ability to be effluxed and its absence of cellular toxicity exhibited by Hoechst 33342- as an identifier for dye efflux associated with putative CSCs. Calcein AM is a cell permeable, non-fluorescent compound which is cleaved by intracellular esterases to produce calcein which fluoresces and is retained in the cytosol.[43] We have identified cells capable of effluxing calcein (calcein low population, $C^{lo}P$) in several human cancer cell lines. $C^{lo}P$ cells are a small subpopulation, though larger than SP, which exhibit significant overlap with SP which has the potential to identify a larger population of putative CSCs. Visualization of cells by fluorescence microscopy using Calcein AM and/or D-luciferin, efflux substrates, in concurrence with Mitotracker Red FM, a mitochondrial dye which is not effluxed, was carried out to identify live cells which possess efflux capability. A novel relationship with p53 inactivation or Bax deletion yielded an enrichment of putative CSCs by our visualization method and was corroborated by flow cytometry. This yields important mechanistic insight into how putative CSCs gain their efflux property which confers MDR.

Results

$C^{lo}P$ overlaps with SP as an identifier of putative CSCs

Hoechst 33342 has been used to identify dye-effluxing SP cells that have been proposed to be CSCs due to their apparently greater tumorigenic potential in vivo.36 Due to the toxicity of Hoechst 33342 at low concentrations and on short time scales,[39] an alternative means of isolating putative CSC's based on dye efflux is desired. To evaluate the feasibilility of Calcein

AM staining as a way of determining dye effluxing cells, the DLD-1 colon carcinoma cell line which has a well described SP was stained with Calcein AM, Hoechst 33342 and PI. Cells were gated for viability based on PI exclusion as well as light scatter (FS and SS). Cells which were viable and considered SP by low Hoechst 33342 fluorescence were quantified as 1.22% and their low fluorescence was inhibited by verapamil, an ABC transporter inhibitor (Fig. 1A). Analyzing fluorescence of calcein yielded a $C^{lo}P$ of 2.17% which was significantly larger than that identified by SP and inhibited by verapamil (Fig. 1B). To assess the overlap of the SP and $C^{lo}P$, SP and non-SP cells were independently analyzed for their $C^{lo}P$ based on the same gating used earlier to determine these subpopulations (Fig. 1C). The SP was determined to have a $C^{lo}P$ of 45.22% and has a strong overall shift to lower calcein fluorescence intensity throughout the population compared to that of the non-SP which contained a $C^{lo}P$ of 1.64%. A number of human cancer cell lines including RKO, DLD-1, MDA-MB-231, SW620 and SW480 were found to contain a $C^{lo}P$ (Fig. 1D). The imperfect but significant overlap of $C^{lo}P$ and SP is likely due to irreversible Hoechst 33342 binding to the minor grove of DNA while the fluorescence of calcein does not require binding.[38,43] Thus putative CSCs which do not efflux Hoechst 33342 before it binds irreversibly are not identified via the SP identification method but would be contained in the $C^{lo}P$ as calcein is not bound. The identification of a larger $C^{lo}P$ relative to SP while exhibiting significant overlap suggests that the $C^{lo}P$ could potentially serve as a better identifier for the putative CSC dye effluxing subpopulations due to their unique respective dye properties.

Calcein AM is non-toxic to cells in contrast to Hoechst 33342

With the observation of a $C^{lo}P$, the toxicities of the dyes were evaluated. To evaluate levels of p53, a transcription factor which regulates many cellular processes such as cell cycle progression after DNA damage, transcriptional activity was determined by a luciferase reporter assay in HCT116 cells treated with varying concentrations of Hoechst 33342 (0–10 μg/mL) at several time points (0–36 h) (Fig. 2A and B). It is clear that Hoechst 33342 increases levels of p53-mediated transcription in a time and dose dependent manner. The decrease in activity at 24 and 36 h is due to apoptosis. To assess the effects of Calcein AM staining as well as Hoechst 33342 staining on cell stress, levels of phosphorylated p53 (serine15) were determined by western blot in the H460 cell line which also expresses WT p53 (Fig. 2C). At both concentrations, Hoechst 33342 staining induced significant levels of phosphorylated p53 (serine 15) whereas Calcein AM staining demonstrated levels close to the control. We then investigated the ability of cells to proliferate following prototypical staining with Hoechst 33342 and Calcein AM. DLD-1 cells were plated at a concentration of 70,000 cells/mL and treated with Hoechst 33342 or Calcein AM at a working concentration of 5 μg/mL for 1.5 h or 50 nM for 2 h, respectively, as defined by their protocols. The stained populations were allowed to proliferate for 10 d and were then fixed and stained with Coomassie blue to visualize cell colonies (Fig. 2D). Markedly, Hoechst 33342 staining yielded no viable cells whereas Calcein AM staining yielded a population close to that of the control. Furthermore, levels of apoptosis were determined by flow cytometry analysis of sub-G1 content following incubation with Hoechst 33342 or Calcein AM at the noted time points and concentrations in HCT116 and DLD-1 cell lines (Fig. 2E). Calcein AM at a 50 nM working concentration displayed levels of apoptosis similar to control cells that were maintained under identical conditions in the absence of fluorescent dye. At 200 nM, Calcein AM produced a modest increase in levels of apoptosis; however it should be remarked that these levels are still less than those of Hoechst 33342 staining under any conditions tested. At both concentrations (5 μg/mL and 20 μg/ mL) of Hoechst 33342, levels of apoptosis were clearly elevated at all time points and in all cell lines tested relative to the control as well as Calcein AM. Lastly, the effects of Calcein AM staining on proliferation was quantitatively determined over several days in DLD-1, SW260, RKO and SW480 cell lines (Fig. 2F). It appears there is a slight lag phase during the first day but overall proliferation is similar to control levels. Taking this evidence together with previous

observations, Calcein AM appears suitable as a nontoxic alternative fluorescent dye that is effluxed by and therefore a potential indicator of putative CSCs.

Luciferin exhibits strong UV-excited fluorescence that can be imaged at a cellular resolution and spatially overlaps with calcein

D-luciferin is a known substrate of ABC transporters[47] which have been associated with SP cells[48] and subsequently implicated in putative CSCs. Due to its strong fluorescence signal and availability, it is employed in a variety of both in vitro and in vivo assays.[47,49] Such studies include screening for ABC transporter inhibitors by means of determining efficacy based on luciferin retention. These studies assume the properties of the sorted populations to be dye-independent. Considering this, conclusions drawn from these studies about subpopulations based on dye-efflux must be taken with caution as differences may be caused by dye-induced alterations of cell cycling, differential toxicity and protein levels/status such as p53, ATM or Chk2.[39] For these reasons, we carried out image analysis of D-luciferin in DLD-1 cells that yielded visualization at cellular resolution not previously achieved. The cells were incubated with D-luciferin for 1 h followed by washing twice with PBS and imaged in PBS + 2 mM $MgCL_2/CaCL_2$ to maintain cell adhesion. These procedures along with a minimal concentration of 250 g/mL of D-luciferin allowed cell visualization of dye-containing cells (Fig. 3B) while higher concentrations yielded diminishing margins in image contrast improvement (Fig. 3C and D). Concentrations below this did not provide a desirable cellular resolution (Fig. 3A). Previous efforts employing D-luciferin lack cellular resolution and rely on bulk signal and fall subject to the previously outlined problems. The demonstrated capability of such resolution could be used in combination with viability stains and other fluorescent probes to visualize the level of dye-retention as well as other important cell properties in a simultaneous, noninvasive and dynamic fashion unparalleled by bulk-signal methods.

Visualization of $ALDH^+$ population and inhibition by DEAB

To further expand our efforts to provide an alternative and improved method for studying putative CSCs under relatively physiological conditions, we explored the use of ALDH activity within putative CSCs as a means to visualize such cells. In addition to dye efflux, ALDH activity has been positively correlated with tumorigenicity[50] and therefore has been suggested as a property of putative CSCs. Thus, we attempted to visualize ALDH activity in DLD-1 human colon carcinoma cells. Cells were stained with Mitotracker Red FM and Aldefluor, a fluorescent probe of ALDH activity, in the described manner and imaged (Fig. 4A). As all cells exhibited significant levels ALDH activity, a threshold was set for visualization of Aldefluor fluorescence so that only cells with higher than average ALDH activity display fluorescence in the image for clarity. DEAB, an inhibitor of ALDH, was added to the media and incubated at 37°C in 5% CO_2 for 1.5 h and imaged in the same field of view (Fig. 4B). It is evident in Figure 4B that ALDH activity is inhibited by DEAB. Images were taken in an identical manner without addition of DEAB to demonstrate Aldefluor fluorescence is not being quenched by photobleaching (Fig. 4C and D). This capability demonstrated in this observation underscores the ability to capture dynamic information concerning cellular properties of putative CSCs. This method can be extended to time lapse studies that observe putative CSCs in real time; however caution is warranted with regards to exposure time and photobleaching.

Visualization of putative CSC populations induced upon p53 inactivation or Bax deletion using fluorescence microscopy and non-toxic dyes

We hypothesized that loss of the p53 tumor suppressor or the pro-apoptotic Bax gene may allow for enrichment of putative CSCs as these genes are often affected in cancer and thus may be involved in the CSC phenotype. Evidence for the transcriptional regulation of some MDR genes by p53 in addition to disease prognosis dependency on the status of these apoptotic genes

in different models also led us to this hypothesis.[13–15,22,51–55] With the demonstrated visualization methods we then searched for putative CSCs in cell lines harboring these genetic aberrancies. The colon carcinoma cell lines mutant p53-expressing DLD-1, WT p53-expressing HCT116, $p53^{-/-}$ HCT116 and $Bax^{-/-}$ HCT116 were analyzed for potential CSC populations via the described putative CSC staining and visualization methods. As demonstrated in WT HCT116 by Figure 5A, cells were stained with Mitotracker Red FM (Fig. 5A, ii), Calcein AM (Fig. 5A, iii) and D-luciferin (Fig. 5A, iv). Cells were imaged, assigned pseudo-color and overlayed (Fig. 5A, i) for analysis. Visual analysis revealed a small dye-effluxing population in DLD-1 cells (Fig. 5D) which was absent in WT HCT116 cells. This observation is in full agreement with published data regarding the SP of these two cell lines.[35] It should also be noted that these putative CSCs have a smaller size than the rest of the population which is a property that has been linked to stem cells.[56] Scrutinizing these images for $Bax^{-/-}$ (Fig. 5B) and $p53^{-/-}$ (Fig. 5C) HCT116 cell lines, a rare dye-effluxing population was noted. In accordance with our hypothesis, these observations suggest a novel relationship between the putative CSC property of dye-efflux and p53 as well as the pro-apoptotic gene Bax. DLD-1, which has an established SP and herein demonstrated $C^{lo}P$, harbors mutant p53 while WT HCT116 has WT p53. Thus it appears p53 inactivation, by mutation or gene deletion, gives rise to the putative CSC property of small molecule efflux. This is consistent with the notion that p53 represses MDR genes that provide detoxifying activity to enhance survival of stem cell populations, and that loss of p53 promotes the CSC phenotype in part at the level of small molecule efflux. The observation that $Bax^{-/-}$ HCT116 appears to have an SP as opposed to WT HCT116 provides evidence for a dependency of the CSC phenotype of dye-efflux on Bax as well. In summary, our method of visualizing CSC properties has suggested a novel relationship of p53 inactivation as well as Bax deletion with the induction of putative CSCs.

Putative CSC populations induced upon p53 inactivation or Bax deletion in colon cancer cell lines

The observation that dye-effluxing capabilities can be induced with inactivation of p53 or through Bax gene deletion is of mechanistic importance to CSCs and merits quantitative validation. To corroborate this assertion we performed SP analysis on DLD-1, WT HCT116, $p53^{-/-}$HCT116 and $Bax^{-/-}$ HCT116 cells. Cells were prepared for analysis by the procedure outlined in the methods section and analyzed by flow cytometry for SP as determined by low Hoechst 33342 fluorescence in viable cells and efflux inhibition by verapamil. In agreement with our previous observations, DLD-1 yielded a significant SP population of 1.47% (Fig. 6A) while WT HCT116 had a negligible SP (Fig. 6B). Moreover, $Bax^{-/-}$ HCT116 had a SP of 0.74% (Fig. 6C) and $p53^{-/-}$ HCT116 had a SP of 0.79% (Fig. 6D) in agreement with qualitative observations by our visualization methods. Infection by an adenovirus vector, Ad-LacZ, in HCT116 $p53^{-/-}$ caused no appreciable change in SP (Fig. 6E) but expression of WT p53 via the adenovirus vector Ad-p53 returned the SP to background levels (Fig. 6F). It should be noted that SP populations are sensitive to their environment[35] and so while the quantification varies in the literature, to our knowledge a relationship of SP induction within a non-SP cell line by gene-deletion has not been previously reported.

Discussion

The relationship of p53 mutations or deletion as well as Bax deletion with putative CSCs provides mechanistic insight for understanding the aberrancies that differentiate CSCs from other cells. Previous studies have been confounded by isolation methods that utilize markers which are not exclusive qualifiers and/or employ toxic dyes to purify these putative CSC populations. The latter in the case of Hoechst 33342 has been shown to be toxic to all subpopulations at low concentrations relative to established protocols. The evidence that Calcein AM stains subpopulations in a non-toxic manner which allows for subsequent

proliferation presents a viable possibility to surmount this impediment. The novel $C^{lo}P$ identified in several cancer cell lines using this method also potentially presents a more accurate identification of dye-effluxing putative CSCs because calcein is localized in the cytosol[43] whereas Hoechst 33342 binds to the minor groove of DNA.[40] Using the staining method as a paradigm, other putative CSC properties could potentially be assayed with the ability to visualize cells in culture and in vivo. This concept is exemplified within this study by fluorescently probing ALDH activity. High ALDH activity has been posited as putative marker for tumorigenicity and has been extended to CSCs[7] and can now be visualized as exhibited by this study. Visualization of D-luciferin at a cellular resolution is unprecedented and has the potential to further elucidate diffidence pertaining to criticism of in vivo studies regarding subpopulation properties being induced by dye-toxicity effects in dye-retaining cells.

It should be noted that due to the limited availability of cell lines with gene knockouts which allows for isogenic comparisons, the enrichment of putative CSCs in this study has been observed exclusively in the colon carcinoma cell line HCT116. Establishing the presented putative CSC enrichment relationship should be extended to other cell lines to corroborate this relationship and/ or expose a deeper understanding of the dependency. For the same purposes, visualization of properties such as calcein efflux and $ALDH^+$ activity visualization should be carried out on other cell lines. Recent evidence has emerged regarding the effects of fluorescent probes on gene expression profiles.[39] Therefore, future studies on identification of putative CSC properties should examine effects on protein expression profiles and cell cycle to limit induced alterations in cellular properties due to the method.

The impact of this work is in providing novel methods for visualization, isolation and tracking of dye-effluxing putative CSC populations in culture and could be extended to in vivo. This has not previously been possible in live cell populations and allows for dynamic monitoring. A range of options is provided by our studies for use of Calcein AM, D-luciferin and ALDH as markers for putative CSC visualization. Such methods can certainly be combined with analysis of cell surface markers by live cell immunofluorescence for further understanding the relationships between various CSC markers and phenotypes associated with cancer development and progression. Future studies can analyze the tumorigenicity of the $C^{lo}P$, herein identified in cancer cell lines possessing dye-effluxing properties associated with putative CSCs in a wide range of human tumor types. The described identification method allows for non-toxic sorting of cancer cell lines based on this property and subsequent evaluation of tumorigenicity in vivo.

An important aspect of our work is the demonstration that loss of the p53 tumor suppressor or the pro-apoptotic Bax genes results in enrichment of putative CSC populations by our analytical methods. In agreement with this novel p53 relationship, reintroduction of WT p53 eliminated these putative CSC populations which concurs with the previously noted p53 regulation of MDR genes such as MDR1 and MRP1.13,15,53–55 While this work was being conducted, a number of studies were published which identified the loss of p53 as a promoter of more efficient reprogramming of differentiated cells into pluripotent cells, or induced pluripotent stem cells (iPS).[57–61] This along with our finding regarding loss of p53 as a promoter of MDR properties highlights the importance of p53 loss of function in conferring putative CSC phenotypic properties. The ability to visualize and track putative CSC populations should facilitate a host of cell culture and in vivo studies regarding cancer progression as well as novel therapy development, including the discovery and testing of agents that may directly target putative CSC populations. Such visualization of putative CSC populations in vivo may be coupled with cell death visualization, e.g., using fluorescently labeled Annexin V, to assess at cellular resolution the effects of specific therapies on CSC and non-CSC in the context of the tumor microenvironment.

Materials and Methods

Cell culture

All tumor cell lines were obtained from the American Type Culture Corporation (ATCC) except $Bax^{-/-}$ HCT116 and $p53^{-/-}$ cell lines which were provided by B. Vogelstein (Johns Hopkins University, Baltimore) and H460 which was from S.B. Baylin (Johns Hopkins University, Baltimore, MD). WT HCT116, $Bax^{-/-}$ HCT116 and $p53^{-/-}$ HCT116 cell lines were grown in McCoy's 5A medium with 10% FBS and 1% Penicillin/ Streptomycin at 37°C in 5% CO_2. DLD-1, RKO, SW480, SW620 and DMAMB-231 cell lines were grown in DMEM (Gibco) with 10% FBS and 1% Penicillin/Streptomycin at 37°C in 5% CO_2. The H460 cell line was grown in RPMI (Gibco) with 10% FBS and 1% Penicillin/Streptomycin at 37°C in 5% CO_2.

Fluorescent dyes

The following fluorescent dyes were used in flow cytometry and/or fluorescence microscopy experiments and the wavelength of light used for excitation (Ex) as well as the wavelength of light collected (Em) is noted parenthetically. Propidium iodide (PI) (488 nm Ex, 675 nm Em) was used exclusively in flow cytometry and was obtained from Sigma-Aldrich (St. Louis, MO). D-Luciferin (Ex 365 nm, Em 450) was obtained from Gold Biotechnology (St. Louis, MO). The fluorescent dyes Mitotracker Red FM (Ex 540 nm, Em 605 nm), Hoechst 33342 (Ex 365 nm, Em 450 nm) and Calcein AM (Ex 480 nm, Em 535 nm) were obtained from Invitrogen (Carlsbad, CA). Mitotracker Red FM was used for staining at a working concentration of 400 nM in all experiments unless otherwise indicated. Calcein AM was used at a working concentration of 50 nM in all experiments unless otherwise indicated. Aldefluor (Ex 480 nm, Em 535 nm) and DEAB were obtained from the ALDEFLUOR Kit from Stem Cell Technologies (Vancouver, BC, CA), and used at concentrations described by the ALDEFLUOR kit protocol.

Luciferase reporter assay

HCT116 cells previously engineered to express a firefly luciferase gene under the control of 13 p53-response elements were treated with Hoechst 33342 at indicated concentrations.[44] Intensities of firefly luciferase activity were imaged and measured as previously described at indicated time points.

Adenovirus preparation and infection

We prepared replication-deficient adenovirus recombinants expressing wild-type p53 (Adp53) and -galactosidase (AdLacZ) as previously described.[45] Determination of viral titers and multiplicity of infection (MOI) for the infected cell line has been described.46 HCT116 $p53^{-/-}$ cells were infected at a MOI of 50.

Western blot analysis

Western blotting was carried out according to standard procedures, using horseradish peroxidase-conjugated secondary antibodies (Santa Cruz Biotechnology, Santa Cruz, CA) and the ECL_+ detection system (Amersham, Arlington Heights, IL). The following antibodies were used: rabbit polyclonal antibodies against phosphorylated serine 15 of p53 at a dilution of 1:1,000 from Cell Signaling Technology (Beverly, MA); mouse monoclonal antibodies against Ran at a dilution of 1:10,000 from BD Technologies (Franklin Lakes, NJ).

Coomassie stain and growth assay

To visualize proliferation after dye staining, cells were plated at a density of 70,000 cells/mL in 3–100 mm × 20 mm cell culture dishes and stained with Hoechst 33342 for 1.5 h at 5 g/mL

working concentration, Calcein AM at a 50 nM working concentration, or only media as a control. After staining, the dye-containing media was aspirated and replaced with fresh media containing no dye. Cells were incubated at 37°C in 5% CO_2 for 10 d, replacing with fresh media once every 3 d. At the end of this 10 d period, cells were washed in PBS and fixed in a solution of 10% methanol and 10% acetate for 5 min. Cells were then stained with Coomassie blue for 5 min and imaged. To quantitatively determine the effect of Calcein AM staining on cell proliferation a growth assay was performed. Cultured cells were treated with Calcein AM (50 nM in growth media) for 30 min at 37°C and 5% CO_2. The cells were washed and incubated with fresh complete medium for the indicated number of days. Cell counts were taken just prior to treatment and at the indicated times after treatment by trypan blue exclusion assay for living cells. Results are expressed as total cell number over time.

SP and $C^{lo}P$ assays by flow cytometry

Flow cytometry was performed using an Elite ESP flow cytometer (Beckman-Coulter, Miami, FL). To analyze the SP, a solid state 355 nm UV laser (Lightwave Electronics, Mt. View, CA) was used to excite the Hoechst 33342 and the dual emission was captured with a 450 nm band pass filter (Hoechst Blue) and a 675 nm band pass filter (Hoechst Red) separated with a 550LP dichroic. Forward scatter (FS) and PI (675/40BP) were captured from a 488 nm argon laser 40 sec upstream of the UV laser. For quantification of SP by flow cytometry, cells were grown to ~70% confluency and were harvested using trypsin (Gibco). Cells were washed and resuspended in cold HBSS (Gibco) at a concentration of 1×10^6 cells/mL containing Hoechst 33342 (5 g/mL) (Invitrogen) for 1.5 h at 37°C, vortexing gently every 30 min. A negative control sample was treated with verapamil (Sigma) (50 M) for 15 min at room temperature prior to the addition of Hoechst 33342. After the incubation with Hoechst 33342, cells were centrifuged, washed, and resuspended in ~300 L HBSS containing PI (2 g/mL). Dead cells were gated out based on PI fluorescence at 675 nm as well as FS and side scatter (SS). $C^{lo}P$ cells were analyzed in the same manner but instead of Hoechst 33342 fluorescence, calcein fluorescence was collected at 520 nm.

Sub-G_1 analysis

PI staining and analysis by flow cytometry were used to quantify the levels of apoptosis induced by Hoechst 33342 and Calcein AM in the indicated cell lines, dye concentrations and time points. Cells were grown to ~70% confluency in 6-well plates, washed with PBS, and digested by 1 mL trypsin at 37°C for 5 min. Cells were washed with 2 mL PBS/1% FBS, resuspended in 0.5 mL PBS. Resuspended cells were added drop-wise into 5 mL cold 70% ethanol with gentle vortexing, then kept on ice for 30 min. Fixed cells were spun down to remove ethanol, washed with 2 ml PBS/1% FBS, and resuspended in 1.0 mL PBS. 0.5 mL of phosphate-citrate buffer (pH 7.8) was then added and the solution was incubated for 5 min. Cells were spun down, resuspended in 300 L PI/RNase staining solution, and stored for 30 min at room temperature in the dark and subsequently analyzed by flow cytometry. Staining with Calcein AM was carried out by the described methods.

Fluorescence microscopy and images

Fluorescence microscopy images were recorded by a QImaging 2000R Camera on an Axiovert 100 inverted microscope. Images were collected and processed using iVision-Mac (BioVision Technologies, Exton, PA). During imaging, cells were maintained by the LiveCell™ system (Pathology Devices, Westminster, MD) at 37°C and 5% CO_2.

Abbreviations

CSC cancer stem cell

SP	side population
$C^{lo}P$	calcein low population
AML	acute myeloid leukemia
ALDH	aldehyde dehydrogenase
ABC	ATP binding cassette
MDR	multidrug resistance
FS	forward scatter
SS	side scatter
WT	wild-type
P-gp	P-glycoprotein

Acknowledgments

This work was supported in part by NIH Grant U54 CA105008 and by the Littlefield-AACR Grant in Metastatic Colon Cancer Research. W.S.E.-D. is an American Cancer Society Research Professor.

References

1. Sell S. Stem cell origin of cancer and differentiation therapy. Crit Rev Oncol/Hematol 2004;51:1–28.
2. Bergsagel DE, Valeriote FA. Growth characteristics of a mouse plasma cell tumor. Cancer Res 1968;28:2187–2196. [PubMed: 5723963]
3. Bruce WR, Van Der Gaag H. A quantitative assay for the number of murine lymphoma cells capable of proliferation in vivo. Nature 1963;199:79–80. [PubMed: 14047954]
4. Haase D, Feuring-Buske M, Konemann S, Fonatsch C, Troff C, Verbeek W, et al. Evidence for malignant transformation in acute myeloid leukemia at the level of early hematopoietic stem cells by cytogenetic analysis of $CD34^+$ subpopulations. Blood 1995;86:2906–2912. [PubMed: 7579382]
5. Mehrotra B, George TI, Kavanau K, Avet-Loiseau H, Moore D 2nd, Willman CL, et al. Cytogenetically aberrant cells in the stem cell compartment ($CD34^+$lin) in acute myeloid leukemia. Blood 1995;86:1139–1147. [PubMed: 7542497]
6. Dick DBJE. Human acute myeloid leukemia is organized as a hierarchy that originates from a primitive hematopoietic cell. Nature Med 1997;3:730–737. [PubMed: 9212098]
7. Singh SK, Hawkins C, Clarke ID, Squire JA, Bayani J, Hide T, et al. Identification of human brain tumour initiating cells. Nature 2004;432:396–401. [PubMed: 15549107]
8. Al-Hajj M, Wicha MS, Benito-Hernandez A, Morrison SJ, Clarke MF. Prospective identification of tumorigenic breast cancer cells. Proc Natl Acad Sci USA 2003;100:3983–3988. [PubMed: 12629218]
9. Huang EH, Hynes MJ, Zhang T, Ginestier C, Dontu G, Appelman H, et al. Aldehyde dehydrogenase 1 is a marker for normal and malignant human colonic stem cells (SC) and tracks SC overpopulation during colon tumorigenesis. Cancer Res 2009;69:3382–3389. [PubMed: 19336570]
10. Hadnagy A, Gaboury L, Beaulieu R, Balicki D. SP analysis may be used to identify cancer stem cell populations. Exp Cell Res 2006;312:3701–3710. [PubMed: 17046749]
11. Goodell MA, Brose K, Paradis GA, Conner S, Mulligan RC. Isolation and functional properties of murine ematopoietic stem cells that are replicating in vivo. J Exp Med 1996;183:1797–1806. [PubMed: 8666936]
12. Hirschmann-Jax C, Foster AE, Wulf GG, Nuchtern JG, Jax TW, Gobel U, et al. A distinct “side population” of cells with high drug efflux capacity in human tumor cells. Proc Natl Acad Sci USA 2004;101:14228–14233. [PubMed: 15381773]
13. Chin KV, Ueda K, Pastan I, Gottesman MM. Modulation of activity of the promoter of the human MDR1 gene by Ras and p53. Science 1992;255:459–462. [PubMed: 1346476]

14. Angelis PD, Stokke L, Smedshammer R, Lothe A, Lehne G, Chen Y, et al. P-glycoprotein is not expressed in a majority of colorectal carcinomas and is not regulated by mutant p53 in vivo. Br J Cancer 1995;72:307–311. [PubMed: 7640210]
15. Sullivan GF, Yang J-M, Vassil A, Yang J, Bash-Babula J, Hait WN. Regulation of expression of the multidrug resistance protein MRP1 by p53 in human prostate cancer cells. J Clin Invest 2000;105:1261–1267. [PubMed: 10792001]
16. Bahr O, Wick W, Weller M. Modulation of MDR/MRP by wild-type and mutant p53. J Clin Invest 2001;107:643–645. [PubMed: 11238567]
17. Schmitt CA, Fridman JS, Yang M, Lee S, Baranov E, Hoffman RM, et al. A senescence program controlled by p53 and $p16^{INK4a}$ contributes to the outcome of cancer therapy. Cell 2002;109:335–346. [PubMed: 12015983]
18. Schmitt CA, Rosenthal CT, Lowe SW. Genetic analysis of chemoresistance in primary murine lymphomas. Nature Med 2000;6:1029–1035. [PubMed: 10973324]
19. Schmitt CA, Fridman JS, Yang M, Baranov E, Hoffman RM, Lowe SW. Dissecting p53 tumor suppressor functions in vivo. Cancer Cell 2002;1:289–298. [PubMed: 12086865]
20. Sparreboom A, Loos WJ, Burger H, Sissung TM, Verweij J, Figg WD, et al. Effect of ABCG2 genotype on the oral vioavailability of topotecan. Cancer Biol Ther 2005;4:650–653. [PubMed: 15908806]
21. Chen Z-S, Robey RW, Belinsky MG, Shchaveleva I, Ren X-Q, Sugimoto Y, et al. Transport of methotrexate, methotrexate polyglutamates and 17{beta}-estradiol 17-({beta}-D-glucuronide) by ABCG2: Effects of acquired mutations at R482 on methotrexate transport. Cancer Res 2003;63:4048–4054. [PubMed: 12874005]
22. Green H, Soderkvist P, Rosenberg P, Horvath G, Peterson C. mdr-1 single nucleotide polymorphisms in ovarian cancer tissue: G2677T/A correlates with response to paclitaxel chemotherapy. Clin Cancer Res 2006;12:854–859. [PubMed: 16467099]
23. Burger H, van Tol H, Boersma AWM, Brok M, Wiemer EAC, Stoter G, et al. Imatinib mesylate (STI571) is a substrate for the breast cancer resistance protein (BCRP)/ABCG2 drug pump. Blood 2004;104:2940–2942. [PubMed: 15251980]
24. Juliano RL, Ling V. A surface glycoprotein modulating drug permeability in Chinese hamster ovary cell mutants. Biochimica et Biophysica Acta (BBA)—Biomembranes 1976;455:152–162.
25. Wu C, Wei Q, Utomo V, Nadesan P, Whetstone H, Kandel R, et al. Side population cells isolated from mesenchymal neoplasms have tumor initiating potential. Cancer Res 2007;67:8216–8222. [PubMed: 17804735]
26. Szotek PP, Pieretti-Vanmarcke R, Masiakos PT, Dinulescu DM, Connolly D, Foster R, et al. Ovarian cancer side population defines cells with stem celllike characteristics and mullerian inhibiting substance responsiveness. Proc Natl Acad Sci USA 2006;103:11154–11159. [PubMed: 16849428]
27. Wulf GG, Luo KL, Jackson KA, Brenner MK, Goodell MA. Cells of the hepatic side population contribute to liver regeneration and can be replenished with bone marrow stem cells. Haematologica 2003;88:368–378. [PubMed: 12681963]
28. Montanaro F, Liadaki K, Volinski J, Flint A, Kunkel LM. Skeletal muscle engraftment potential of adult mouse skin side population cells. Proc Natl Acad Sci USA 2003;100:9336–9341. [PubMed: 12886022]
29. Pearce DJ, Ridler CM, Simpson C, Bonnet D. Multiparameter analysis of murine bone marrow side population cells. Blood 2004;103:2541–2546. [PubMed: 14644998]
30. Asakura A, Seale P, Girgis-Gabardo A, Rudnicki MA. Myogenic specification of side population cells in skeletal muscle. J Cell Biol 2002;159:123–134. [PubMed: 12379804]
31. Welm BE, Tepera SB, Venezia T, Graubert TA, Rosen JM, Goodell MA. Sca-1pos cells in the mouse mammary gland represent an enriched progenitor cell population. Dev Biol 2002;245:42–56. [PubMed: 11969254]
32. Falciatori I, Borsellino G, Haliassos N, Boitani C, Corallini S, Battistini L, et al. Identification and enrichment of spermatogonial stem cells displaying side-population phenotype in immature mouse testis. FASEB J 2004;18:376–378. [PubMed: 14688197]
33. Yano S, Ito Y, Fujimoto M, Hamazaki TS, Tamaki K, Okochi H. Characterization and localization of side population cells in mouse skin. Stem Cells 2005;23:834–841. [PubMed: 15917479]

34. Ayako M, Yumi M, Ayano K, Takuya S, Hideyuki O. Flow cytometric analysis of neural stem cells in the developing and adult mouse brain. J Neurosci Res 2002;69:83747.
35. Tavaluc RT, Hart LS, Dicker DT, El-Deiry WS. Effects of low confluency, serum starvation and hypoxia on the side population of cancer cell lines. Cell Cycle 2007;6:2554–2562. [PubMed: 17912032]
36. Kondo T, Setoguchi T, Taga T. Persistence of a small subpopulation of cancer stem-like cells in the C6 glioma cell line. Proc Natl Acad Sci USA 2004;101:781–786. [PubMed: 14711994]
37. Patrawala L, Calhoun T, Schneider-Broussard R, Zhou J, Claypool K, Tang DG. Side population is enriched in tumorigenic, stem-like cancer cells, whereas $ABCG2^{+}$ and $ABCG2^{-}$ cancer cells are similarly tumorigenic. Cancer Res 2005;65:6207–6219. [PubMed: 16024622]
38. Chen AY, Yu C, Bodley A, Peng LF, Liu LF. A new mammalian DNA topoisomerase I poison hoechst 33342: Cytotoxicity and drug resistance in human cell cultures. Cancer Res 1993;53:1332–1337. [PubMed: 8383008]
39. Hong Z, Frank T, Jurek D, Donald W, Zbigniew D. Induction of DNA damage response by the supravital probes of nucleic acids. Cytometry Part A 2009;75:510–519.
40. Chen AY, Yu C, Gatto B, Liu LF. DNA minor groove-binding ligands: a different class of mammalian DNA topoisomerase I inhibitors. Proc Natl Acad Sci USA 1993;90:8131–8135. [PubMed: 7690143]
41. Leemhuis T, Yoder MC, Grigsby S, Agüero B, Eder P, Srour EF. Isolation of primitive human bone marrow hematopoietic progenitor cells using hoechst 33342 and rhodamine 123. Exp Hematol 1996;24:1215–1224. [PubMed: 8765497]
42. Zhou S, Schuetz JD, Bunting KD, Colapietro AN, Sampath J, Morris JJ, et al. The ABC transporter Bcrp1/ABCG2 is expressed in a wide variety of stem cells and is a molecular determinant of the side-population phenotype. Nature Med 2001;7:1028–1034. [PubMed: 11533706]
43. Braut-Boucher F, Pichon J, Rat P, Adolphe M, Aubery M, Font J. A non-isotopic, highly sensitive, fluorimetric, cell-cell adhesion microplate assay using calcein AM-labeled lymphocytes. J Immunol Meth 1995;178:41–51.
44. Wang W, El-Deiry WS. Bioluminescent molecular imaging of endogenous and exogenous p53-mediated transcription in vitro and in vivo using an HCT116 human colon carcinoma xenograft model. Cancer Biol Ther 2003;2:196–202. [PubMed: 12750563]
45. El-Deiry WS, Tokino T, Velculescu VE, Levy DB, Parsons R, Trent JM, et al. WAF1, a potential mediator of p53 tumor suppression. Cell 1993;75:817–825. [PubMed: 8242752]
46. Sax JK, Dash BC, Hong R, Dicker DT, El-Deiry WS. The cyclin-dependent kinase inhibitor butyrolactone is a potent inhibitor of $p21^{WAF1/CIP1}$ expression. Cell Cycle 2002;1:87–93.
47. Zhang Y, Bressler JP, Neal J, Lal B, Bhang H-EC, Laterra J, Pomper MG. ABCG2/BCRP expression modulates D-Luciferin based bioluminescence imaging. Cancer Res 2007;67:9389–9397. [PubMed: 17909048]
48. Summer R, Kotton DN, Sun X, Ma B, Fitzsimmons K, Fine A. Side population cells and Bcrp1 expression in lung. Am J Physiol Lung Cell Mol Physiol 2003;285:97–104.
49. Zhang Y, Byun Y, Ren YR, Liu JO, Laterra J, Pomper MG. Identification of inhibitors of ABCG2 by a bioluminescence imaging-based high-throughput assay. Cancer Res 2009;69:5867–5875. [PubMed: 19567678]
50. Christ O, Lucke K, Imren S, Leung K, Hamilton M, Eaves A, et al. Improved purification of hematopoietic stem cells based on their elevated aldehyde dehydrogenase activity. Haematologica 2007;92:1165–1172. [PubMed: 17666374]
51. Park YB, Kim HS, Oh JH, Lee SH. The co-expression of p53 protein and P-glycoprotein is correlated to a poor prognosis in osteosarcoma. Int Orthopaedics 2001;24:307–310.
52. van der Zee AG, Hollema H, Suurmeijer AJ, Krans M, Sluiter WJ, Willemse PH, et al. Value of P-glycoprotein, glutathione S-transferase pi, c-erbB-2 and p53 as prognostic factors in ovarian carcinomas. J Clin Oncol 1995;13:70–78. [PubMed: 7799045]
53. Vilgelm A, Wei JX, Piazuelo MB, Washington MK, Prassolov V, El-Rifai W, Zaika A. [Delta]Np73 [alpha] regulates MDR1 expression by inhibiting p53 function. Oncogene 2007;27:2170–2176. [PubMed: 17952118]
54. Bush JA, Li G. Regulation of the Mdr1 isoforms in a p53-deficient mouse model. Carcinogenesis 2002;23:1603–1607. [PubMed: 12376467]

55. Johnson RA, Ince TA. Scotto KW Transcriptional repression by p53 through direct binding to a novel DNA element. J Biol Chem 2001;276:27716–27720. [PubMed: 11350951]

56. Cintia SDP, Stephen CP, De-Quan L. Cell size correlates with phenotype and proliferative capacity in human corneal epithelial cells. Stem Cells 2006;24:368–375. [PubMed: 16123387]

57. Marion RM, Strati K, Li H, Murga M, Blanco R, Ortega S, et al. A p53-mediated DNA damage response limits reprogramming to ensure iPS cell genomic integrity. Nature 2009;460:1149–1153. [PubMed: 19668189]

58. Utikal J, Polo JM, Stadtfeld M, Maherali N, Kulalert W, Walsh RM, et al. Immortalization eliminates a roadblock during cellular reprogramming into iPS cells. Nature 2009;460:1145–1148. [PubMed: 19668190]

59. Kawamura T, Suzuki J, Wang YV, Menendez S, Morera LB, Raya A, et al. Linking the p53 tumour suppressor pathway to somatic cell reprogramming. Nature 2009;460:1140–1144. [PubMed: 19668186]

60. Hong H, Takahashi K, Ichisaka T, Aoi T, Kanagawa O, Nakagawa M, et al. Suppression of induced pluripotent stem cell generation by the p53-p21 pathway. Nature 2009;460:1132–1135. [PubMed: 19668191]

61. Li H, Collado M, Villasante A, Strati K, Ortega S, Canamero M, et al. The Ink4/Arf locus is a barrier for iPS cell reprogramming. Nature 2009;460:1136–1139. [PubMed: 19668188]

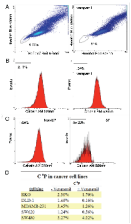

Figure 1.

Analysis of SP and $C^{lo}P$ by flow cytometry in cell lines treated with Calcein AM and Hoechst 33342. Dead cells were first gated out based on FS and SS as well as PI staining. SP cells were identified by its low Hoechst 33342 fluorescence and its efflux inhibition by verapamil treatment (A). After gating out dead cells, the $C^{lo}P$ was also quantified in the total population based on its low calcein fluorescence and its efflux inhibition by verapamil treatment (B). To determine the overlap of SP and $C^{lo}P$, the $C^{lo}P$ was quantified for non-SP and SP (C) as determined by the gate for SP shown in (A). A significant $C^{lo}P$ was identified in a number of human cancer cell lines (D).

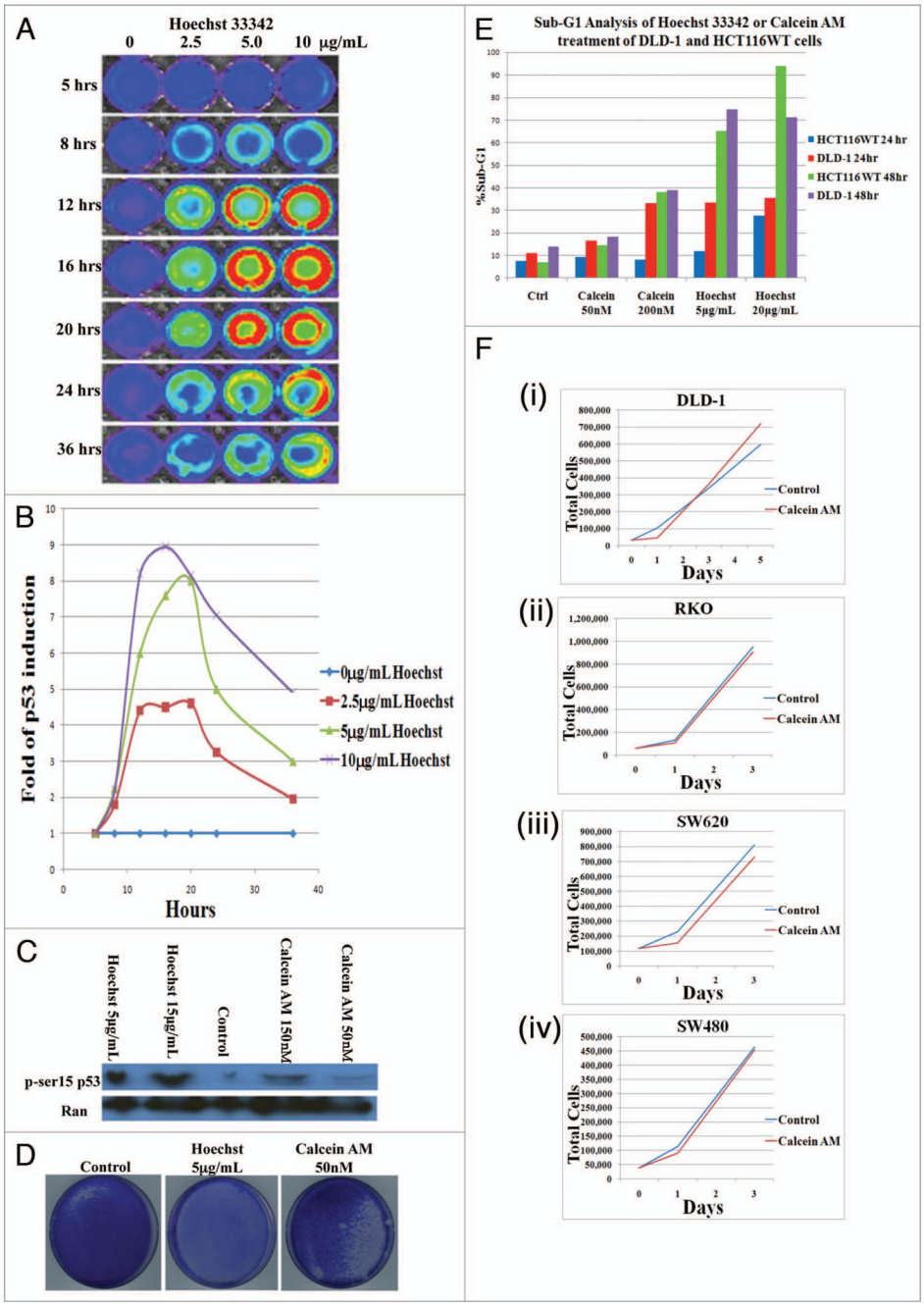

Figure 2.

Hoechst 33342 induces cell stress and death while Calcein AM does not. HCT116 cells containing a p53 luciferase reporter shows an induction of p53 mediated transcriptional activity in a dose and time dependent manner with hoechst 33342 treatment (A and B). H460 cells were treated with Hoechst 33342 for 1.5 h or Calcein AM for 2 h at indicated concentrations and protein expression level of phospho-p53 (ser15) were determined by western blot (C). Coomassie stain after 10 d following plating at 70,000 cells/mL and treatment with Hoechst 33342 for 1.5 h or Calcein AM for 2 h at indicated concentrations (D). sub-G_1 analysis by flow cytometry following incubation of DLD-1 or HCT116 cells with Hoechst 33342 or Calcein

AM at indicated concentrations after 24 or 48 h incubation (E). proliferation of DLD-1 (i), RKO (ii), SW620 (iii) or SW480 (iv) cell lines following Calcein AM staining (F).

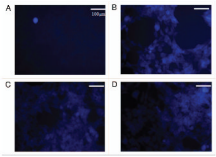

Figure 3.
Fluorescence imaging of D-luciferin in the DLD-1 cell line at various concentrations of D-luciferin. Concentrations of D-luciferin were imaged at 50 μg/mL (a), 250 μg/mL (B), 500 μg/mL (C) and 750 μg/mL (D). The optimal concentration was determined to be 250 μg/mL which provided cellular resolution after washing with PBS.

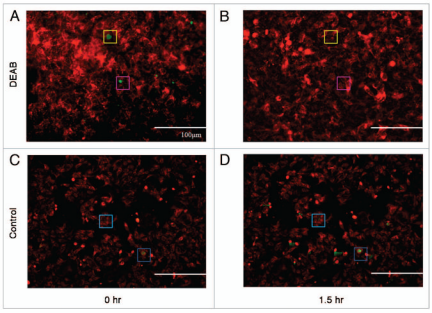

Figure 4.

Visualization by fluorescence microscopy of an $ALDH^+$ population and its inhibition. DLD-1 cells were stained with Aldefluor and imaged in the same field of view before (A) and 1.5 h after the addition of DEAB (B). DLD-1 cells were stained with Aldefluor and imaged in the same field of view before (C) and 1.5 h after staining as a control for fluorescence quenching or photobleaching (D). Boxes of the same color show identical locations in the field of view as reference point for locating $ALDH^+$ cells. To emphasize putative CsCs expressing high aLDh activity, a threshold level was set so that only cells expressing higher than average Aldefluor fluorescence are shown in green. Mitotracker Red FM was used as a counterstain before Aldefluor staining and is shown in red.

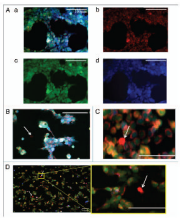

Figure 5.

Visualization of dye effluxing population. Visualization of fluorescence in viable WT HCT116 cells (A) showing Mitotracker Red FM (red) (b), calcein (green) (c), D-luciferin (blue) (d) and an overlay (a). The same staining was carried out in (B) $Bax^{-/-}$ HCT116, (C) $p53^{-/-}$ HCT116, and (D) DLD-1 cell lines. Dye-effluxing cells are indicated by white arrows. All scales bars are 100 m.

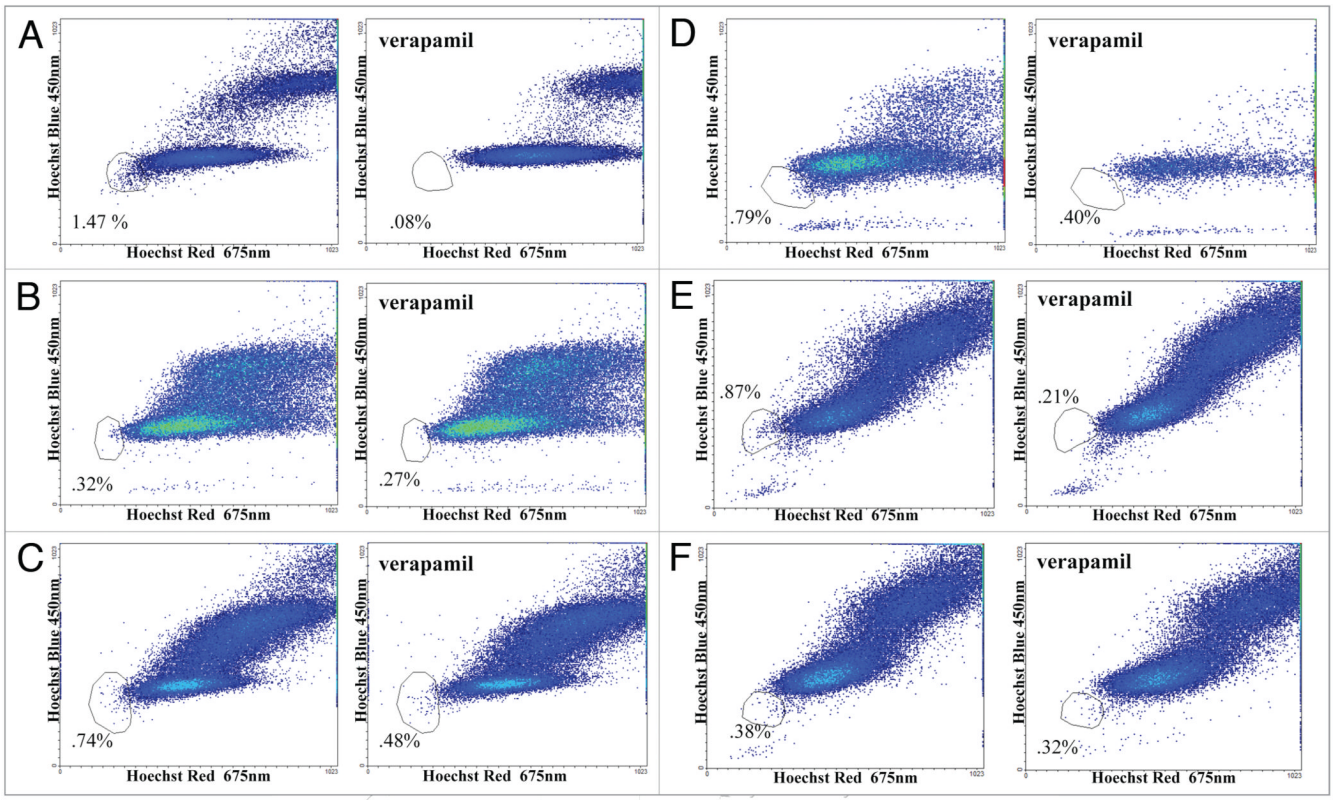

Figure 6.

Quantification of SP using Hoechst 33342 staining by flow cytometry in colon carcinoma cell lines with different p53 and/or Bax gene status. SP were determined in (a) DLD-1 (mutant p53), (B) HCT116 (WT p53), (C) HCT116 $Bax^{-/-}$ and (D) HCT116 $p53^{-/-}$ cell lines. Noting the induction of SP upon Bax deletion or p53 inactivation, SP were then determined following the overexpression of p53 using (E) Ad-LacZ as a control and (F) Ad-p53 in HCT116 $p53^{-/-}$ to confirm the relationship between p53 and dye-effluxing properties.